MFI zeolite coating with intrazeolitic aluminum (acidic) gradient supported on SiC foams to improve the methanol-to-propylene (MTP) reaction

Yilai Jiao[a,b,c], Shaojun Xu[b], Chunhai Jiang[d], Michal Perdjon[c], Xiaolei Fan[b,*], Jinsong Zhang[a,*]

[a] Shenyang National Laboratory for Materials Science, Institute of Metal Research, Chinese Academy of Sciences, 72 Wenhua Road, Shenyang 110016, China
[b] School of Chemical Engineering and Analytical Science, The University of Manchester, Oxford Road, Manchester, M13 9PL, United Kingdom
[c] Cardiff Catalysis Institute, School of Chemistry, Cardiff University, Park Place, Cardiff, CF10 3AT, United Kingdom
[d] Institute of Advanced Energy Materials, School of Materials Science and Engineering, Xiamen University of Technology, and Key Laboratory of Functional Materials and Applications of Fujian Province, 600 Ligong Road, Xiamen 361024, China

ARTICLE INFO

Keywords:
MFI zeolite
Methanol-to-propylene (MTP)
SiC foam
Aluminum gradient
Anti-coking

ABSTRACT

To hinder the deactivation and improve the propylene selectivity in the methanol-to-propylene (MTP) reaction, MFI coating with the intrazeolitic aluminum (acidic) gradient supported on SiC foam support (G-MFI/SiC foam) was proposed. The solid polycrystalline silicon was used in the synthesis of G-MFI/SiC foam catalyst provided a prolonged release of silica nutrient in the liquid phase and suppressed the precipitation phenomena. The re-sulting MFI coating showed the aluminum gradient along the surface normal direction of SiC foams with ZSM-5 layer (about 20 μm) near the SiC surface followed by the silicalite-1 layer (about 10 μm). The alumina (acidic) gradient in the MFI coating renders a passive outer layer of silicalite-1 with fairly large amount of weak and medium acid sites prevented the coke formation as well as promoted the selectivity to propylene in the MTP reaction. Compared to the conventional ZSM-5/SiC foam catalyst, the G-MFI/SiC foam catalyst showed excellent performance in the MTP reaction with good catalytic longevity (8 h vs. 76 h for > 95% methanol conversion) and low coke deposition (6.7×10^{-3} wt.% h^{-1} vs. 0.26 wt.% h^{-1}), as well as high propylene selectivity (ca. 36% vs. 46%).

1. Introduction

Propylene is one of the most-produced building blocks (e.g. for the production of polypropylene) in the petrochemical industry with an estimated global demand at 94.2 million tons in 2015 [1,2]. Propylene was traditionally produced as the by-products of petrochemical cracking processes (e.g. steam cracking and fluid catalytic cracking), which cannot fill the projected propylene gap in the market (i.e. about 20 million tons in 2020 [3]). The reconfiguration of cracking processes to enhance the propylene production is challenging due to the con-straints in the operation and the high energy consumption of crackers [3]. Over the past 15 years, the development of on-purpose propylene production technologies such as olefin metathesis [4] and alcohols to propylene [5] has attracted the attention of academia as well as in-dustry as the solution to increase the propylene supply.

The conversion of methanol to propylene, the so-called MTP process [5–9], represents an innovative way to make propylene overcoming the historical barrier against using natural gas or coal to make olefins [1]. However, there are few technical challenges in the MTP process that need to be addressed to mature the technology for its confident adoption by industry. The MTP reaction is catalyzed by framework catalysts, such as SAPO-34 [10–12] and ZSM-5 [13–18] zeolites with strong exothermicity ($_{r}H° \approx -45$ kJ mol^{-1}), and hence the elimina-tion of the temperature gradient and the adiabatic temperature rise across the bed is necessary [15,18]. In addition, the selectivity of the MTP reaction and the deactivation of framework catalysts are highly influenced by the global and local mass transfer steps [13,14,17].

Recent development of the structured catalysts such as pure zeolite monoliths [16] and zeolites supported on cellular foam catalysts [14,18–23], especially structured catalysts based on silicon carbide (SiC) foams, provided innovative solutions to overcome the heat and mass transfer limitations in MTP reactions. The combination of the intrinsic physical/chemical properties of SiC (e.g. high chemical re-sistance, high thermal conductivity and low linear expansion coeffi-cient) [14,20–22,24–28] and geometrical characteristics of open-cell foams (e.g. high permeability, low pressure drop, high mechanical strength and enhanced axial and radial mixing) [26,28–35] has been demonstrated to be effective for promoting various reactions, including methanol to dimethyl ether and MTP reactions [12,14,18–22,25,36,37].

* Corresponding authors.
E-mail addresses: xiaolei.fan@manchester.ac.uk (X. Fan), jshzhang@imr.ac.cn (J. Zhang).

Macroscopically, framework catalysts are assembled as the thin coating on the surface of SiC foams (via dip-coating [18], direct hy-drothermal [14,19–22] or microwave-assisted synthesis [12,27]), which provides the reactants with easy access to the active sites and reduces the limitation of global mass transfer [14,18,21,22]. Ad-ditionally, the uniform temperature distribution across the foam bed was also achieved due to the good heat transfer property of SiC [18]. Mesoscopically, the inter-crystal porous structure and the distribution of acid sites in the zeolite coating need to be tuned carefully to suppress the by-product formation (e.g. ethane and butanes) as well as to prevent the deactivation by coking.

The diffusion of MTP products through the zeolite coating to the bulk media can be generally facilitated by the creation of intercrystal mesopores in the zeolite coating [18]. However, the uniform distribu-tion of acid sites across the entire coating is prone to promote the side reactions and to initiate the coke formation, as well as compromising the selectivity to propylene [38–41]. For bulk zeolites, recent research has shown that the core-shell configuration of zeolite crystals (i.e. acidic H-ZSM-5 zeolite core with a catalytically inert silicalite-1 shell) [42] was able to improve the para-xylene selectivity significantly (> 99%) in the methanol to hydrocarbon reaction. Stimulated by this strategy, we hypothesized that the presence of the intrazeolitic acid gradient (i.e. high aluminum concentration near the SiC wall and low aluminum concentration at the external layer of the coating) across the zeolite assembly could also enhance the performance of the zeolite/SiC foams catalysts in the MTP reaction by preventing the coke formation at the external surface of the zeolite coating.

It was known that, in the direct coating synthesis, the zeolite coating was developed consecutively from the formation of a continuous gel phase on the support followed by the subsequent zeolite nucleation and crystallization [43], which were affected by the nutrient supply and the synthesis time. Therefore, crucial aspects of synthesizing zeolite coating with the aluminum gradient on SiC foams are to (i) selectively form the aluminosilicalite gel on the support (for initiating the formation of zeolite layer with a relatively high aluminum concentration) at the initial stage of synthesis and (ii) control the supply of silica nutrients in the liquid phase (for inhibiting the aluminosilicalite gel formation in the liquid phase and tuning the acid sites across the assembly).

Previously, we have shown that the use of a solid silica source of polycrystalline silicon (in the preparation of silicalite-1 coating on SiC foam supports) was able to achieve the prolonged release of silica source (via the dissolution of polycrystalline silicon in alkaline solu-tions) to suppress the homogenous nucleation in the solution [44,45]. By combining the exploitation of the surface residual silicon of SiC struts, which facilitates the formation of aluminosilicalite gel layer on the surface of SiC struts at the early stage of crystallization, the con-struction of the zeolite coating on SiC foams with the intrazeolitic acid gradient should be feasible.

Herein, we present a synthesis strategy which employs the surface residual silicon of SiC foams and solid polycrystalline silicon to achieve the selective and controlled supply of silica nutrients, as well as using the alumina nutrient in the liquid phase to promote the initial alumi-nosilicate layer on the surface of SiC struts, for the preparation of MFI zeolite coating on SiC foam supports with the aluminum gradient, i.e. the decreased intrazeolitic concentration of alumina across the coating from the SiC surface to the outer surface of the coating. The effect of the synthesis time at a fixed synthesis temperature of 443 K on the forma-tion of the aluminum gradient in the MFI zeolite coating was in-vestigated. The developed structured catalysts were assessed using the MTP reaction in a packed foam reactor. The relevant catalytic perfor-mance in terms of the methanol conversion, propylene selectivity and coke formation were analyzed to demonstrate the superiority of the MFI zeolite coating with the intrazeolitic alumina gradient over the con-ventional MFI coating.

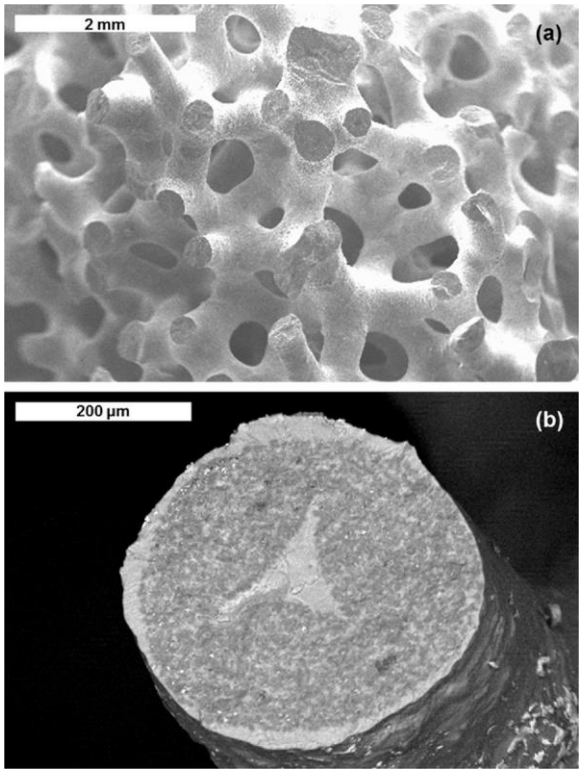

Fig. 1. SEM micrographs of open cell SiC foams: (a) microstructure of the open-cell SiC foam and (b) the cross section of the SiC strut.

2. Experimental

2.1. Open-cell SiC foams

SiC foam supports were fabricated by the controlled reaction bonding and sintering method, as described in our previous publica-tions [44–46]. The scanning electron microscope (SEM) images of the as-prepared SiC foam ceramic supports are shown in Fig. 1. The three-dimensional (3-D) reticulated SiC foams possess evenly distributed and well-connected millimeter-scale open pores (> 500 μm with ca. 70% open-cell porosity, Fig. 1a). The cross-section of a SiC strut is shown in Fig. 1b displaying the surface residual silicon (ca. 5 wt.%) in the SiC phase. The residual silicon can be used as the silicon nutrient to pro-mote the strong anchorage of zeolite phase on the surface of SiC foams [44,45].

2.2. Preparation of MFI-type zeolite coating on SiC foams (MFI/SiC foam)

All chemicals were purchased from the Sinopharm Chemical Reagent Co., Ltd and used as received. The synthesis solution to grow MFI zeolites on SiC foams was prepared by mixing tetra-propylammonium bromide (TPABr, 98%), sodium hydroxide (NaOH, 98%), Aluminum nitrate ($Al(NO_3)_3$, 98%) and deionized water with a molar composition of $Al(NO_3)_3$:TPABr:NaOH:H_2O = 0.12:3:3:750. In this work, polycrystalline silicon was used to achieve the prolonged release of silica nutrients to the liquid phase. The syntheses were per-formed in autoclave reactors with 100 mL Teflon liners.

The typical procedure of synthesis was to: (i) add the SiC foam support (10 mL volume) in the Teflon liner on a Teflon support; (ii) add polycrystalline silicon particles (1 g, diameters: 0.84–1.65 mm) to the Teflon liner; (iii) charge the liner with the synthesis solution (50 mL) to immerse the SiC foam; and (iv) seal the Teflon-lined stainless steel au-toclave and heat it at 443 K for various reaction times (0–96 h) under hydrostatic conditions. After the hydrothermal synthesis, MFI/SiC foam

composites were washed thoroughly with hot water and dried at 373 K in air. The samples were subsequently calcined at 823 K for 8 h to re-move the organics from the zeolite framework.

2.3. Characterization of materials

MFI/SiC foams composites were characterized by X-ray diffraction (XRD, Rigaku Ultima IV, Japan, CuKα_1 radiation, 30 kV, 15 mA, λ = 1.5406 Å, 5° < 2θ < 80°, step size = 0.02° and step time = 2 s, the sample was scanned as a whole), scanning electron microscopy-energy dispersive X-ray spectroscopy (SEM-EDX, Zeiss SUPRA 35, Germany, 9 kV accelerating voltage, in the SEM-EDX analysis of the cross section of the sample, the sample was embedded in the epoxy resin first, then cut and polished prior to the analysis), ammonia tem-perature-programmed desorption (NH_3-TPD, Micromeritics AutoChem II 2920 chemisorption analyzer, 10 K min^{-1} under He flow, details of the TPD analysis is available in our previous work [22], structured catalysts were grinded into particles of 30–40 mesh, acidities were de-termined based on the mass of the composite) and nitrogen (N_2) ad-sorption-desorption measurement at 77 K (Micromeritics 3Flex Surface Characterization Analyzer, pretreatment conditions: 1 h at 363 K then 6 h at 623 K, Brunauer–Emmett–Teller, BET, values were reproducible to ± 7%). The trace element of aluminum and silicon from the filtrate of synthesis solutions was analyzed by the inductively coupled plasma optical emission spectroscopy (ICP-OES, Optima 7300 V HF, the acid digestion method was used with HNO_3, HCl and HF to dissolve zeo-lites). The thermogravimetry analysis (TGA) of spent catalysts was performed on a TG analyzer (Pyris Diamond TG/DTA, PerkinElmer) at a heating rate of 10 K min^{-1} from 300 to 800 K in air (20 mL min^{-1}).

2.4. Methanol-to-propylene (MTP) reaction

The methanol-to-propylene (MTP) reaction was performed in a micro packed foam bed reactor (inner diameter = 26 mm). For each experiment, one piece of cylindrical zeolite/SiC foam catalyst (dia-meter = 25 mm, length = 24 mm) and HPLC grade methanol (≥99.9%, Sinopharm Chemical Reagent Co., Ltd) were used. MTP re-actions were carried out under conditions of 743 K, 0.1 MPa and me-thanol weight hourly space velocity (WHSV, methanol mass flow rate divided by the weight of MFI zeolite coating) of 3 h^{-1}. The product distribution of hydrocarbons and dimethylether (including the un-reacted methanol) was analyzed by a GC (Agilent 7890 A GC) equipped with a PoraPLOT Q column (fused silica ID = 0.32 mm and length = 50 m) and a flame ionization detector (FID). The calculation of the conversion of methanol and the selectivity was described in our previous publication [22].

3. Results and discussion

3.1. Synthesis of MFI-type zeolite coating on SiC foams

The hydrothermal synthesis of MFI-type zeolite coating on SiC foams was carried out using polycrystalline silicon as the silica nutrient. The evolution of the MFI zeolite phase on SiC foams was studied qua-litatively by XRD (Fig. 2). The XRD patterns of the MFI/SiC foam composites at various times during the synthesis are shown in Fig. 2a, in which the development of the MFI coating is a function of the synthesis time. The presence of silicon in the original SiC foam supports was confirmed by the diffraction peaks at 2θ = 28.4°, 47.4°, and 56.1° corresponding to the Si(1 1 1), Si(2 2 0), and Si(3 1 1) surfaces, re-spectively. With the progress of the synthesis, the diffraction peaks of the silicon phase in SiC foams disappeared after 6 h, indicating the dissolution of the surface silicon by the alkaline synthesis solution. The resulting local high concentration of silica nutrient near the SiC strut could promote the selective formation of cross-linked silica-alumina gel on the surface of SiC foams by consuming the alumina nutrient in the

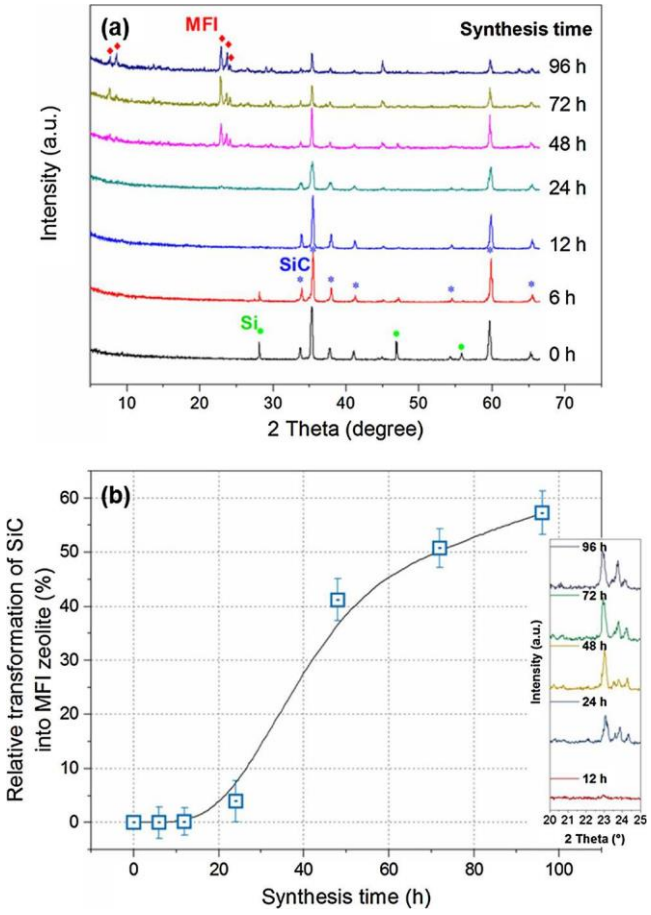

Fig. 2. (a) Powder XRD patterns of MFI/SiC foam composites (in absolute counts); (b) Relative transformation of SiC into MFI zeolite coatings as a function of synthesis time. Inset: Enlarged diffractograms in the 20–25° range for MFI zeolite phase on SiC foams.

liquid phase. It is worth noting that, in the XRD experiment, the coated foam was scanned as a whole, rather than grinded into powders, in order to observe the evolution of the surface silicon on the SiC foam during the synthesis.

As the synthesis proceeded, the MFI zeolite phase gradually devel-oped. After 24 h of synthesis, the typical XRD reflection of the MFI structure emerged, i.e. the doublet at 2θ = 7.9° and 8.9° and triplets in the range of 2θ = 23–25°, and the relative intensity rose gradually with an increase in the synthesis time. The relative transformation of SiC into MFI zeolite in the crystallization process can be qualified relatively by comparing the integrated peak areas of the zeolitic phase at the range of 23–24° 2θ to that of the SiC phase at the range of 33.5–38.5° 2θ [45], as shown in Fig. 2b. Due to the dissolution of the surface silicon on SiC foams, a relatively long induction time was observed, i.e. 24 h (relative transformation into MFI phase = 4%). By prolonging the synthesis time from 24 h to 72 h, a steep rise in the relative transformation was noticed indicating the formation of MFI zeolitic phase on the surface of SiC foams. By extending the synthesis time to 96 h, the full coverage of MFI zeolite on SiC surface were achieved (Fig. S1).

The morphological evolution of MFI/SiC foam composites during the synthesis was examined comprehensively by SEM, as shown in Fig. 3. The SEM image of the original SiC foam surface shows the continuous silicon phase with embedded SiC particles (Fig. 3a). After 6 h of synthesis, a dense aluminosilicate gel layer was formed on the surface of the SiC support (Fig. 3b), which was confirmed by the EDX analysis showing the high aluminum concentration of the surface (Si/Al ratio of 3.5). As the synthesis proceeded, the partial dissolution of the surface gel layer was noticed, which was then followed by the

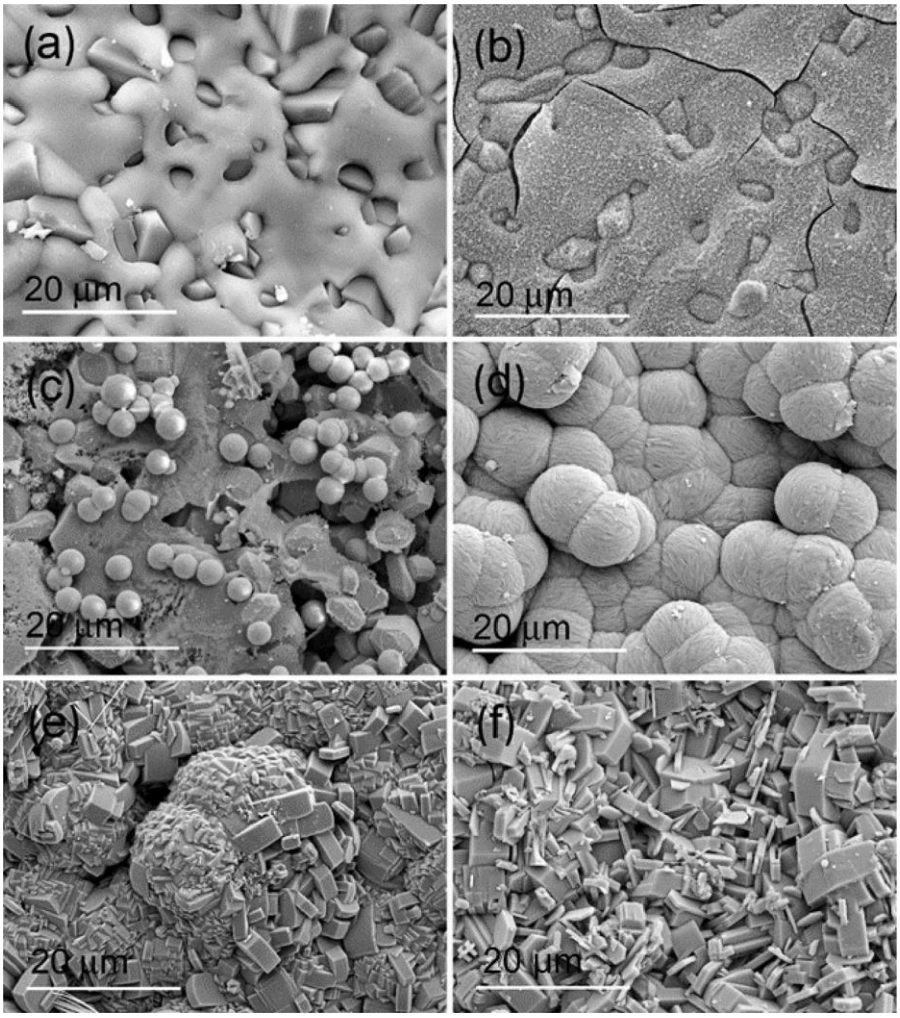

Fig. 3. SEM images of the surface of MFI/SiC foam composites at different synthesis times: (a) 0 h, (b) 6 h, (c) 24 h, (d) 48 h, (e) 72 h, and (f) 96 h.

formation of spherical polycrystalline aggregates (about 3 μm diameter after 24 h, Fig. 3c) with a silicon/aluminum (Si/Al) ratio of 13 (Fig. S2 and Table S1). After 48 h, the SiC surface was fully covered by the spherical polycrystalline aggregates of zeolites (about 10 μm diameter, Fig. 3d). The gradual growth of the zeolite coating was also accom-panied with an increase in its Si/Al ratio (ca. 45, Fig. S2 and Table S1) suggesting the gradual decrease in the Al species in the MFI coating along the surface normal of SiC foams. Further increase in the synthesis time (> 72 h) led to the construction of coffin-shaped MFI crystals with a high Si/Al ratio of 360 (Fig. S2 and Table S1) based on the spherical polycrystalline aggregates (Fig. 3e). The maximum synthesis time used in this work was 96 h, when the whole surface of the SiC foam was covered by coffin-shaped silicalite-1, as evidenced by the surface SEM image of Fig. 3f. The SEM analyses of the cross-sections of samples are presented in Figs. S3 and S4, showing the evolution of MFI zeolitic layer on SiC foam struts over the course of the synthesis. The thicknesses of inner MFI layer with high aluminum concentration and the outer sili-calite-1 layer are about 20 and 10 μm, respectively.

The N_2 adsorption-desorption analyses were carried out to evaluate the porous properties of the MFI/SiC foam composites (Fig. 4). The composites show the characteristic type I N_2 sorption isotherms (i.e. as microporous materials) after 48 h synthesis, whereas the SiC foam support showed negligible micropore volume and surface area (< 1 m^2 g^{-1}). Based on the typical specific micropore volume of 0.175 cm^3 g^{-1} for the MFI zeolite, the amounts of MFI coating in the composites are estimated, as summarized in Table 1, showing that the

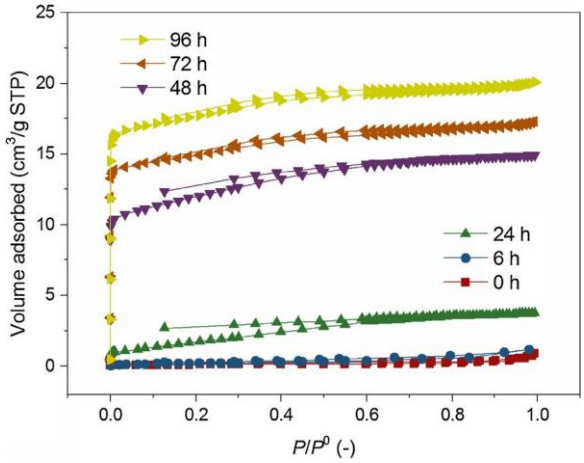

Fig. 4. N_2 adsorption–desorption isotherms of MFI/SiC composites prepared after different synthesis time.

amount of MFI coating is about 12.6 wt.% on SiC foam after 96 h synthesis.

In addition, the mechanical stability of the MFI zeolite coating on SiC foams was also evaluated by the ultrasonic treatment (in water bath for 60 min with 40 KHz frequency), showing the insignificant weight loss (i.e. 0.5 ± 0.3 wt.%) after the sonication.

Table 1
Porous properties of MFI/SiC composites after various synthesis time.

Synthesis time [h]	S_{BET} [$m^2\ g^{-1}$]	S_{micro}[a] [$m^2\ g^{-1}$]	S_{ext}[a] [$m^2\ g^{-1}$]	V_{micro}[a] [$cm^3\ g^{-1}$]	V_t[b] [$cm^3\ g^{-1}$]	Zeolite coating[c] [wt.%]
0	0.4	–[d]	–[d]	–[d]	0.001	–
6	4.2	–[d]	–[d]	–[d]	0.003	–
24	5.8	–[d]	–[d]	–[d]	0.005	–
48	43.6	27.9	15.7	0.012	0.023	6.8
72	54.8	44.0	10.8	0.018	0.027	10.3
96	65.2	52.7	12.5	0.022	0.031	12.6

[a] Determined using the t-plot method.
[b] Single point adsorption total pore volume at $P/P^o = 0.994$.
[c] Determined by N_2 sorption data of V_{micro} values of the bulk MFI zeolite and MFI/SiC foam composites.
[d] Not detectable by N_2 sorption.

3.2. Intra zeolitic aluminum (acidic) gradient across the MFI zeolite coating

The surface EDX analysis of the MFI coating (Fig. S2 and Table S1) showed the first glimpse of the variation of the Si/Al ratio of the MFI layer during the hydrothermal synthesis, suggesting the formation of aluminum gradient along the surface normal of SiC foams. By quanti-fying the element silicon and aluminum in the liquid phase using the ICP-OES (Fig. 5), it was found that the variation of silica and alumina nutrients also supported the hypothesis of aluminum gradient forma-tion across the MFI zeolite layer.

The silica nutrient in the liquid phase showed a rapid increase to ca. 9.3 g L^{-1} at the initial stage of the synthesis (< 6 h), which was asso-ciated with the dissolution of surface silicon from the SiC foam support and polycrystalline silicon. This claim was supported by the negative weight change of MFI/SiC foam composites as shown in Fig. S5 (ca. −2.66 wt.% at the beginning of the hydrothermal synthesis). The silica nutrient in the solution was then consumed by the formation of the aluminosilicate gel layer as well as the subsequent nucleation and crystallization of the zeolite phase, which was proved by the gradual decrease in the Si concentration in the solution after 6 h.

For the alumina nutrient in the liquid phase, the initial drop (< 6 h) was attributed to the gel formation on the SiC surface. On the contrary, at the stage of 6–24 h, aluminum concentration in the liquid phase did not decrease obviously, indicating that the alumina nutrient for the initial zeolite nucleation and crystal growth was provided by the alu-minosilicate gel instead of the alumina nutrient in the liquid phase. The following decrease in the aluminum concentration (24–72 h, to ca. 0.003 g L^{-1}) was caused by the formation of ZSM-5 zeolite, which was also evidenced by the positive weight change of the composite (Fig. S5). After 72 h, the alumina nutrient in the liquid phase was fully depleted. In contrast with the phenomenon observed for the alumina nutrient (> 72 h), the silica nutrient in the liquid still gradually decreased from 6.5 g L^{-1} to 5.1 g L^{-1}, which proved (i) the prolonged release of the silica nutrient by the polycrystalline silicon and (ii) the formation of pure silica MFI zeolite phase (i.e. silicalite-1) on top of the previous ZSM-5 layer, i.e. the formation of MFI coating with the aluminum gradient.

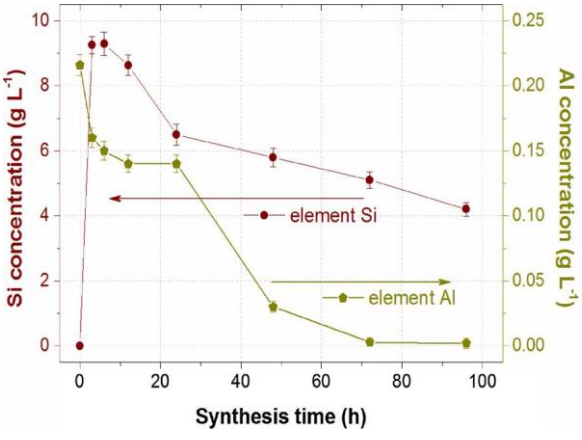

Fig. 5. The element Si and Al concentration in the synthesis solution as the function of the synthesis time.

The dissolution of polycrystalline silicon (solid phase) in the synthesis system was partially compromised by the growth of zeolitic phase on polycrystalline silicon, as evidenced by its surface morphology changes (Fig. S6). The appearing and disappearing of zeolitic phases were found over the course of the synthesis and the latter was attrib-uted to the peeling off of the surface layer due to the dissolution of polycrystalline silicon. The nucleation of zeolite on polycrystalline si-licon was caused by the presence of impurities in it, such as various metal oxides (Fig. S7), which cannot be dissolved by the alkaline so-lution. With extended synthesis hours, zeolite growth dominated leading to the full coverage on polycrystalline silicon by zeolites (e.g. after 96 h, Fig. S6f), as well as stopping the provision of silicon source to the synthesis solution.

In comparison to the conventional hydrothermal synthesis of zeolite coating, the most distinctive feature of the current work is the use of the polycrystalline silicon (solid phase) and liquid alumina source, which resulted in the formation of MFI layered assembly of ZSM-5 (alumina rich) and silicalite-1 (pure silica), i.e. the aluminum gradient across the MFI coating along the surface normal of SiC foams. Based on the characterization of materials above, the following mechanism was proposed for the formation of the aluminum gradient across the MFI coating on SiC foam supports.

At the initial stage of the synthesis, the residual silicon on the sur-face of the SiC foam support was dissolved, which provided a silicon rich region on the surface and encouraged the cross-linking with the alumina nutrient in the solution to form the aluminosilicate gel layer with a high aluminum concentration. Then, the Al-rich aluminosilicate gel layer partially dissolved and nucleated to zeolite crystals with the low Si/Al ratio. As the reaction continued, the growth of zeolite layer gradually depleted alumina nutrient in the liquid phase formed the high aluminum concentration MFI layer (ZSM-5) near the surface. The pro-longed release of silica nutrient by the continuous dissolution of the polycrystalline silicon then contributed to the growth of pure silica MFI layer (silicalite-1) on top of the ZSM-5 layer after exhausting the alu-mina nutrient in the solution. During the synthesis, similar processes were also expected to occur on the surface of polycrystalline silicon particles, and hence the growth of MFI zeolite coating ceased when the entire surface of silicon particles were covered by zeolite crystals.

To demonstrate the effectiveness of the polycrystalline silicon on the creation of the acidic gradient across the MFI layer, a reference com-posite was prepared (under the hydrothermal condition of 443 K for 96 h, aluminum nitrate as the alumina source) using the conventional silica source of tetraethyl orthosilicate (TEOS) [46]. The cross-sectional SEM images of the corresponding MFI/SiC foam struts prepared using different silica sources are shown in Fig. 6. As expected, the poly-crystalline silicon as the silica nutrient promoted a hybrid structure in

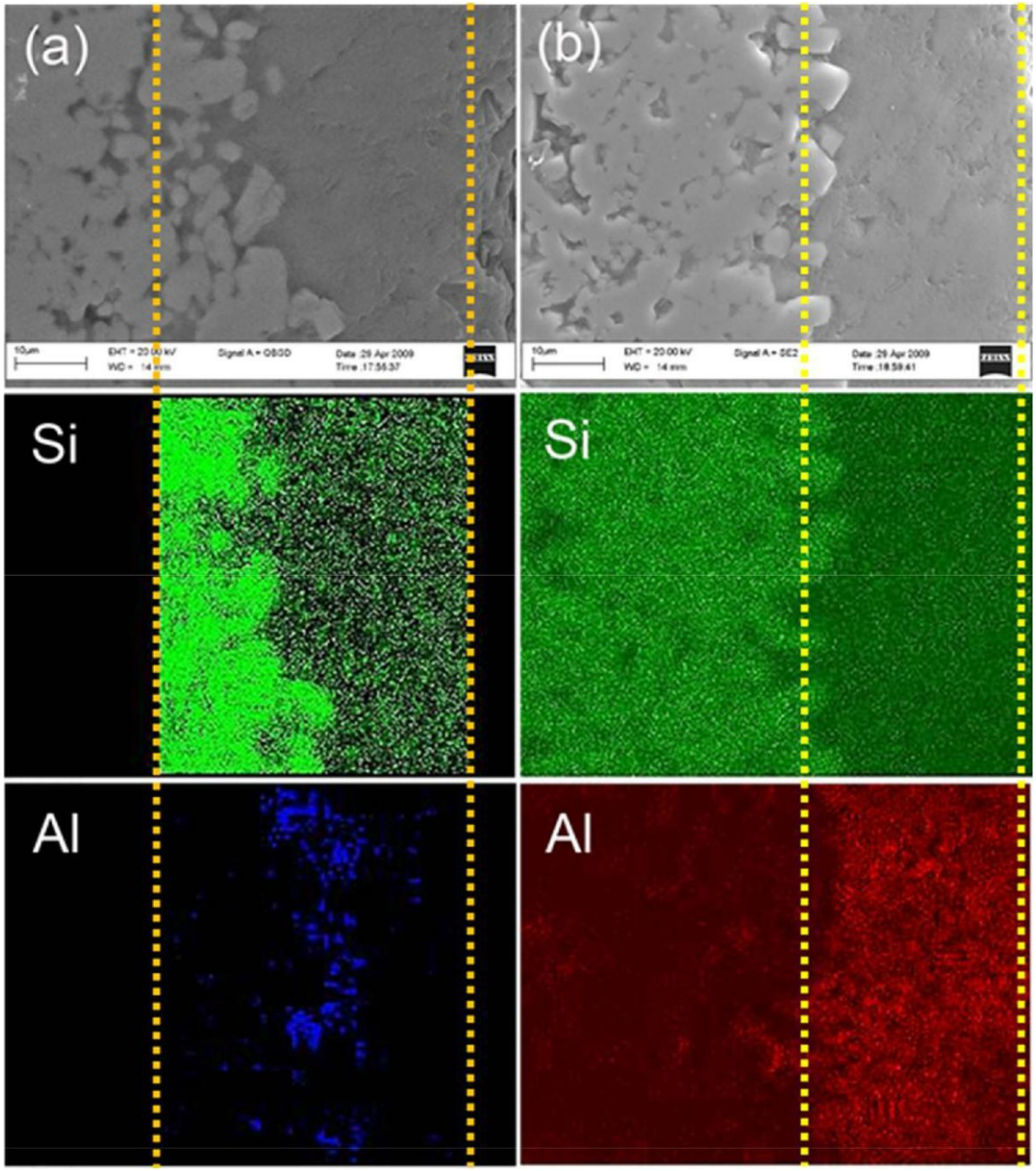

Fig. 6. SEM micrographs and Si and Al EDX mapping of the cross-sectional surface of (a) G-MFI/SiC foam composite with aluminum gradient and (b) ZSM-5/SiC foam composite.

the MFI layer with the high aluminum concentration region in the inner layer of the MFI coating (Fig. 6a, the aluminum gradient). The use of TEOS in the liquid phase, by contrast, led to the conventional ZSM-5 coating on the SiC surface with the uniform alumina phase across the coating layer (Fig. 6b).

In addition, the use of the polycrystalline silicon was also suspected to be able to suppress the precipitation phenomena that were com-monly observed in the conventional system with an excess of nutrients (with respect to the mass needed for the coating) in the liquid phase [43]. In present work, the SEM analysis of materials revealed the non-uniform coverage of MFI coating on SiC struts as the result of con-ventional synthesis with TEOS (Fig. S8a), in which the upper surface of SiC struts was preferably covered by randomly oriented zeolite crystals with size of about $5 \times 10 \times 20\ \mu m^3$. But the coverage of zeolite crystals on bottom of the SiC foam support was very poor, clearly demonstrated the precipitation phenomena that was caused by the fine zeolite crystals formed in the liquid phase. By replacing the TEOS with the poly-crystalline silicon, a dense and well-distributed zeolite coating layer of about 25 μm thick was fabricated on the SiC supports, as shown in Figs. S8b and 6a.

3.3. Catalytic test

Further investigations of the developed structured catalysts in the MTP reaction showed that the acidic gradient across the MFI layer played an important role in improving the performance of the struc-tured catalyst (Fig. 7 and Table 2). For the comparative purpose, the MTP reaction was carried out using the MFI/SiC foam catalysts syn-thesized for 48 h (7 wt.% coating, mainly ZSM-5, Si/Al ratio = 45, de-noted as MFI/SiC-48) and 96 h (12.8 wt.% coating, G- MFI, denoted as

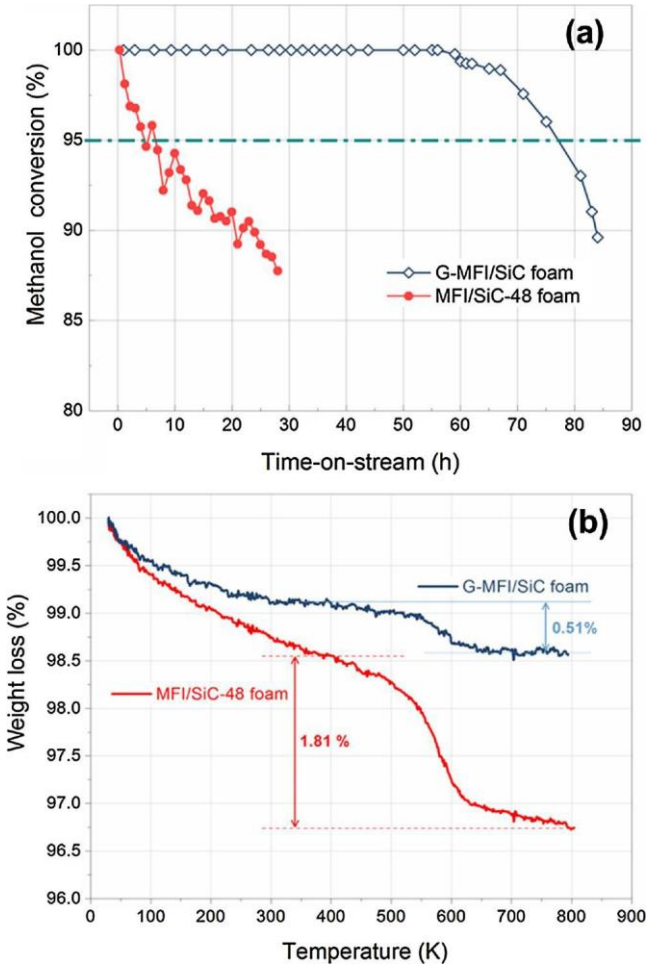

Fig. 7. (a) Methanol conversion as a function of time-on-stream over the struc-tured catalysts (conditions: 743 K; 0.1 MPa; 3 h^{-1} methanol WHSV; for G-MFI/SiC: $F_{nitrogen}$ = 480 cm^3 min^{-1}, $F_{methanol}$ = 0.31 cm^3 min^{-1}, F_{water} = 0.24 cm^3 min^{-1}; for MFI/SiC-48: $F_{nitrogen}$ = 260 cm^3 min^{-1}, $F_{methanol}$ = 0.17 cm^3 min^{-1}, F_{water} = 0.13 cm^3 min^{-1}); (b) weight loss of the spent catalysts from the MTP re-actions in this work.

G-MFI/SiC), respectively, to evaluate the effectiveness of the developed MFI/SiC foam catalyst with the aluminum (acidic) gradient along the surface normal of SiC foams. All MTP experiments were performed at the same WHSV of 3 h^{-1} (based on the mass of zeolite coatings on SiC foam supports, the porous features of the two catalysts are shown in Fig. 4 and Table 1).

G-MFI/SiC showed enhanced catalytic activity (in terms of me-thanol conversion and selectivity to propylene) and catalytic longevity compared to MFI/SiC-48. It was found that the catalytic activity of G-MFI/SiC was highly dependent on the nature of the MFI coatings. G-MFI/SiC remained active with > 95% methanol conversions [16,18,47] for about 76 h, whereas MFI/SiC-48 deactivated after ca. 7 h of time-on-stream (ToS, Fig. 7a).

The difference in catalytic activity could be related to the coke formation in MFI-type coatings during the reaction. After the MTP re-action, the coke deposition of the deactivated catalysts was analyzed by TGA (Fig. 7b). The amount of the coke deposited on G-MFI/SiC corre-sponds to different durations of the methanol conversion since the de-activation occurs at different ToSs (Fig. 7a). By characterizing the weight loss in the temperature range of > 400 K, only ca. 0.51 wt.% was measured for G-MFI/SiC, while about 1.81 wt.% for MFI/SiC-48. By considering the active lifespan of the two catalysts in the MTP reaction, the average coking rate of G-MFI/SiC is significantly slower than that of MFI/SiC-48, i.e. 6.7 × 10^{-3} wt.% h^{-1} vs. 0.26 wt.% h^{-1}. The coke formation caused serious pore closure in the spent MFI/SiC-48, as evidenced by the N_2 sorption analysis of the spent catalysts after the MTP (Figs. S9 and S10). For the MFI/SiC-48 catalyst, the BET surface area dropped by ca. 60% after the MTP (Tables 1 and S2). Conversely, it was only about 10% for the G-MFI/SiC catalyst. Based on the physi-sorption data (Table 1), the intercrystalline macro-mesopores were present in the resulting zeolite coatings on SiC foams. However, since the distinct coke formation was observed in the comparative study, one could conclude that the main benefit from the developed catalyst was due to the Al-gradient in the surface zeolitic coating.

In addition to the enhanced anti-coking ability, the intrazeolitic acidic gradient of the MFI coating was also found beneficial to the se-lectivity to propylene. The product distribution of the MTP reactions is shown in Table 2, in which G-MFI/SiC presents relatively high se-lectivities to propylene as well as low selectivities to aromatics out-performed MFI/SiC-48. Repeated reactions were performed with cata-lyst samples from the same synthesis protocols, showing that the conversion and selectivity values were reproducible to better than ± 5%.

For G-MFI/SiC,the resistance to coke deposition and the enhanced selectivity to propylene are attributed to the alumina (acidic) gradient presented within the MFI layer, in which the passive outer layer of pure silica plays a role in both accounts. NH_3-TPD analysis of the two cata-lysts revealed the nature of acid sites as seen in Fig. 8.

The NH_3-TPD profile of MFI-type coatings showed two kinds of NH_3 desorption regions at 393–473 K and 473–653 K, respectively. The peaks in the first region (Table 3) stems from the desorption of NH_3 from the weak acid sites (SieOH) [48]. By comparing the integrated area of peaks in the region of 393–473 K, the concentration of weak acid sites in the G-MFI coating was about 101% more than that in the ZSM-5 coating, suggesting the excess silica phase in G-MFI/SiC. G-MFI/ SiC only showed desorption peak at around 528 K (strong acid sites), whilst the profile of MFI/SiC-48 showed another NH_3 desorption peak

Table 2
Product selectivities of structured SiC foam catalysts catalyzed MTP reaction.

Catalyst	ToS [h]	Conversion[a] [%]	Selectivity [%]					C_3H_6/C_2H_4
			C_{1-4}	C_2H_4	C_3H_6	C_4H_8	C_5^+	
MFI/SiC-48	6	95.8	8.0	11.5	35.7	17.7	27.1	3.1
	15	92.0	5.7	10.0	37.6	19.1	27.5	3.8
	28	87.7	4.5	9.0	38.6	19.6	28.3	4.3
G-MFI/SiC	3	100	3.0	9.9	46.2	25.9	15.0	4.7
	15	100	3.1	9.3	46.3	25.0	16.2	5.0
	28	100	3.4	8.7	46.4	24.2	17.3	5.4
	56	100	3.8	7.3	45.6	22.4	20.9	6.3
	71	97.6	3.7	6.0	44.8	20.7	24.8	7.5
	84	89.6	3.3	5.5	43.1	20.4	27.8	7.9

[a] Carbon mass balance > 95.0%.

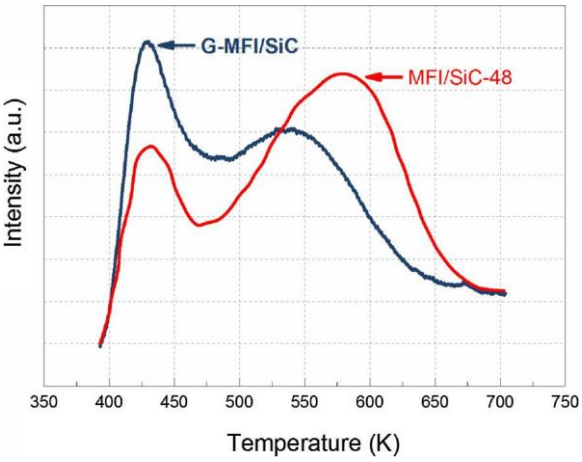

Fig. 8. NH_3-TPD profiles of G-MFI/SiC and MFI/SiC-48.

Table 3
NH_3-TPD data of MFI/SiC foam composites.

Sample	Temperature at maximum [K]		Weak acidity[a] [μmol g^{-1}]	Strong acidity[b,c] [μmol g^{-1}]
	First peak	Second peak		
MFI/SiC-48	433	573	8.0	26.6
G-MFI/SiC	429	528	16.1	18.2

[a] Acidity of the first peak.
[b] Acidity of the second peak.
[c] Acidities on the basis of the mass of the composites.

at 573 K, which is in good agreement with the previously reported strong acid sites in ZSM-5 coating with homogeneous Si/Al framework [18]. Compared to the ZSM-5 coating on SiC foams (MFI/SiC-48), the amount of strong acid sites in the G-MFI coating was reduced by 31.6% (Table 3), indicating the coverage of the ZSM-5 layer by low aluminum concentration silicalite-1 layer in the G-MFI coating.

As discussed above, the alumina (acidic) gradient in the MFI-type zeolite coating renders a passive outer layer of pure silica with less strong acid sites prevented the coke formation. The presence of the acidic gradient along the surface normal of SiC foams was confirmed by SEM-EDX and NH_3-TPD. Compared to the conventional ZSM-5 coating on SiC foam, the reduction in the strong acid sites in the external layer of the coating also prevented the secondary transformation of the active products, especially the aromatization of olefins, leading to the reduced coke formation. Additionally, in comparison to the conventional ZSM-5 coating, the additional weak and medium acid sites created by the alumina (acidic) gradient in G-MFI/SiC facilitated the alkylation [49] and methylation [50] for olefin formation, giving rise to the enhance-ment in propylene selectivity measured in the MTP reaction.

4. Conclusions

In summary, a method was developed to employ the solid silica source of polycrystalline silicon to achieve the prolonged release of the silica source in the synthesis of MFI zeolite coating on SiC foams re-sulted in the formation of the aluminum gradient along the surface normal of SiC foams (with high aluminum concentration in the inner layer and low aluminum concentration in the outer layer).

The initial dissolution of the surface residue silicon on SiC foams formed the aluminosilicate gel on the surface of SiC foams, which en-couraged the subsequent growth of aluminosilicate MFI zeolite layer near the surface by using the alumina source in the liquid phase. The use of polycrystalline silicon provided the prolonged release of the silica source in the liquid phase. Upon the consumption of the alumina source in the liquid phase, a MFI zeolite layer with low aluminum concentration was formed on top of the previous aluminosilicate MFI zeolite layer created the aluminum gradient across the MFI coating. In addition, the use of polycrystalline silicon in the synthesis also pre-vented the excess of silica nutrients in the liquid phase suppressed the crystallization throughout the solution and the precipitation phe-nomena [27,43]. The coating structure resulting from the developed method was confirmed by SEM-EDX analysis.

The presence of the aluminum gradient across the MFI coating re-sulted in the acidic gradient that was beneficial to the MTP reaction by preventing the deactivation. Compared to the conventional ZSM-5/SiC (i.e. MFI/SiC-48 in this work) foam catalyst, the developed G-MFI/SiC foam catalyst exhibited the catalytic enhancement in MTP reaction with good catalytic longevity (8 h vs. 76 h for > 95% methanol conversion), low coke deposition (6.7×10^{-3} wt.% h^{-1} vs. 0.26 wt.% h^{-1}) as well as high propylene selectivity (ca. 36% vs. 46%), thanks to the absence of strong acid sites in the silica-rich outer layer.

Acknowledgements

The authors would like to thank the financial support from the National 863 Program of China (2012AA030304). XF gratefully ac-knowledge financial support from the Engineering and Physical Sciences Research Council for his research (EP/R000670/1). YJ thanks the China Scholarship Council (CSC) for his visiting fellowship in the UK (201604910181). XF and YL also thanks the Higher Education Innovation Funded 'Knowledge and Innovation Hub for Environmental Sustainability' at The University of Manchester for supporting YJ's visit to The University of Manchester.

Appendix A. Supplementary data

Supplementary material related to this article can be found, in the online version, at doi:https://doi.org/10.1016/j.apcata.2018.04.006.

References

[1] J.S. Plotkin, American Chemical Society News, Cutting-Edge Chemistry, The Propylene Gap: How Can It Be Filled? (September 14, 2015). https://www.acs.org/content/acs/en/pressroom/cutting-edge-chemistry/the-propylene-gap-how-can-it-be-filled.html. (Accessed 08 October 2017).
[2] J.S. Plotkin, American Chemical Society News, Cutting-Edge Chemistry, The Propylene Quandary. (August 8, 2016). https://www.acs.org/content/acs/en/pressroom/cutting-edge-chemistry/the-propylene-quandary.html. (Accessed 08 October 2017).
[3] A. Akah, M. Al-Ghrami, Appl. Petrochem. Res. 5 (2015) 377–392.
[4] J.C. Mol, J. Mol. Catal. A: Chem. 213 (2004) 39–45.
[5] M. Stöcker, Microporous Mesoporous Mater. 29 (1999) 3–48.
[6] N.-L. Michels, S. Mitchell, J. Pérez-Ramírez, ACS Catal. 4 (2014) 2409–2417.
[7] L. Borchardt, N.-L. Michels, T. Nowak, S. Mitchell, J. Pérez-Ramírez, Microporous Mesoporous Mater. 208 (2015) 196–202.
[8] A. Galadima, O. Muraza, Ind. Eng. Chem. Res. 54 (2015) 4891–4905.
[9] M. Khanmohammadi, S. Amani, A.B. Garmarudi, A. Niaei, Chin. J. Catal. 37 (2016) 325–339.
[10] G. Yang, Y. Wei, S. Xu, J. Chen, J. Li, Z. Liu, J. Yu, R. Xu, J. Phys. Chem. C 117 (2013) 8214–8222.
[11] Z. Li, J. Martínez-Triguero, J. Yu, A. Corma, J. Catal. 329 (2015) 379–388.
[12] M.M. Elamin, O. Muraza, Z. Malaibari, H. Ba, J.-M. Nhut, C. Pham-Huu, Chem. Eng. J. 274 (2015) 113–122.
[13] Q. Wang, S. Xu, J. Chen, Y. Wei, J. Li, D. Fan, Z. Yu, Y. Qi, Y. He, S. Xu, C. Yuan, Y. Zhou, J. Wang, M. Zhang, B. Su, Z. Liu, RSC Adv. 4 (2014) 21479–21491.
[14] Y. Jiao, X. Yang, C. Jiang, C. Tian, Z. Yang, J. Zhang, J. Catal. 332 (2015) 70–76.
[15] I. Yarulina, F. Kapteijn, J. Gascon, Catal. Sci. Technol. 6 (2016) 5320–5325.
[16] J. Zhou, J. Teng, L. Ren, Y. Wang, Z. Liu, W. Liu, W. Yang, Z. Xie, J. Catal. 340 (2016) 166–176.
[17] P. Losch, A.B. Pinar, M.G. Willinger, K. Soukup, S. Chavan, B. Vincent, P. Pale, B. Louis, J. Catal. 345 (2017) 11–23.
[18] Y. Jiao, X. Fan, M. Perdjon, Z. Yang, J. Zhang, Appl. Catal. A: Gen. 545 (2017) 104–112.
[19] S. Ivanova, B. Louis, B. Madani, J.P. Tessonnier, M.J. Ledoux, C. Pham-Huu, J. Phys. Chem. C 111 (2007) 4368–4374.
[20] Y. Liu, S. Podila, D.L. Nguyen, D. Edouard, P. Nguyen, C. Pham, M.J. Ledoux, C. Pham-Huu, Appl. Catal. A: Gen. 409–410 (2011) 113–121.

[21] Y. Jiao, C. Jiang, Z. Yang, J. Zhang, Microporous Mesoporous Mater. 162 (2012) 152–158.
[22] Y. Jiao, C. Jiang, Z. Yang, J. Liu, J. Zhang, Microporous Mesoporous Mater. 181 (2013) 201–207.
[23] E. Tronconi, G. Groppi, C.G. Visconti, Curr. Opin. Chem. Eng. 5 (2014) 55–67.
[24] S. Ivanova, C. Lebrun, E. Vanhaecke, C. Pham-Huu, B. Louis, J. Catal. 265 (2009) 1–7.
[25] H. Ba, Y. Liu, X. Mu, W.-H. Doh, J.-M. Nhut, P. Granger, C. Pham-Huu, Appl. Catal. A: Gen. 499 (2015) 217–226.
[26] X. Fan, X. Ou, F. Xing, G.A. Turley, P. Denissenko, M.A. Williams, N. Batail, C. Pham, A.A. Lapkin, Catal. Today 278 (Part 2) (2016) 350–360.
[27] X. Ou, S. Xu, J.M. Warnett, S.M. Holmes, A. Zaheer, A.A. Garforth, M.A. Williams, Y. Jiao, X. Fan, Chem. Eng. J. 312 (2017) 1–9.
[28] X. Ou, X. Zhang, T. Lowe, R. Blanc, M.N. Rad, Y. Wang, N. Batail, C. Pham, N. Shokri, A.A. Garforth, P.J. Withers, X. Fan, Mater. Charact. 123 (2017) 20–28.
[29] P. Ciambelli, V. Palma, E. Palo, Catal. Today 155 (2010) 92–100.
[30] V. Palma, A. Ricca, P. Ciambelli, Catal. Today 216 (2013) 30–37.
[31] X. Gao, X. Li, X. Liu, H. Li, Z. Yang, J. Zhang, Chem. Eng. Sci. 135 (2015) 489–500.
[32] H. Li, L. Fu, X. Li, X. Gao, AIChE J. 61 (2015) 4509–4516.
[33] H. Li, F. Wang, C. Wang, X. Gao, X. Li, Chem. Eng. Sci. 123 (2015) 341–349.
[34] X. Li, Q. Liu, H. Li, X. Gao, J. Taiwan Inst. Chem. Eng. 64 (2016) 39–46.
[35] X. Li, Y. Qiao, H. Li, X. Gao, J. Clean. Prod. 133 (2016) 54–64.
[36] L. Truong-Phuoc, T. Truong-Huu, L. Nguyen-Dinh, W. Baaziz, T. Romero, D. Edouard, D. Begin, I. Janowska, C. Pham-Huu, Appl. Catal. A: Gen. 469 (2014) 81–88.
[37] A.N. Kouamé, R. Masson, D. Robert, N. Keller, V. Keller, Catal. Today 209 (2013) 13–20.
[38] S. Müller, Y. Liu, M. Vishnuvarthan, X. Sun, A.C. van Veen, G.L. Haller, M. Sanchez-Sanchez, J.A. Lercher, J. Catal. 325 (2015) 48–59.
[39] L. Qi, J. Li, L. Wang, L. Xu, Z. Liu, Catal. Sci. Technol. 7 (2017) 894–901.
[40] J.S. Martinez-Espin, K. De Wispelaere, M. Westgård Erichsen, S. Svelle, T.V.W. Janssens, V. Van Speybroeck, P. Beato, U. Olsbye, J. Catal. 349 (2017) 136–148.
[41] J. Li, Y. Wang, W. Jia, Z. Xi, H. Chen, Z. Zhu, Z. Hu, J. Energy Chem. 23 (2014) 771–780.
[42] K. Miyake, Y. Hirota, K. Ono, Y. Uchida, S. Tanaka, N. Nishiyama, J. Catal. 342 (2016) 63–66.
[43] J.C. Jansen, J.H. Koegler, H. van Bekkum, H.P.A. Calis, C.M. van den Bleek, F. Kapteijn, J.A. Moulijn, E.R. Geus, N. van der Puil, Microporous Mesoporous Mater. 21 (1998) 213–226.
[44] Y. Jiao, Z. Yang, X. Cao, C. Tian, D. Su, J. Zhang, Chin. J. Mater. Res. 23 (2009) 458–465.
[45] Y. Jiao, Z. Yang, J. Zhang, Chin. J. Mater. Res. 24 (2010) 25–32.
[46] Y. Jiao, Z. Yang, X. Cao, C. Tian, Y. Gao, J. Zhang, Rare Met. Mater. Eng. 38 (2009) 286–288.
[47] S. Zhang, Y. Gong, L. Zhang, Y. Liu, T. Dou, J. Xu, F. Deng, Fuel Process. Technol. 129 (2015) 130–138.
[48] B. Liu, L. France, C. Wu, Z. Jiang, V.L. Kuznetsov, H.A. Al-Megren, M. Al-Kinany, S.A. Aldrees, T. Xiao, P.P. Edwards, Chem. Sci. 6 (2015) 5152–5163.
[49] Q. Zhu, J.N. Kondo, T. Setoyama, M. Yamaguchi, K. Domen, T. Tatsumi, Chem. Commun. (2008) 5164–5166.
[50] W. Wu, W. Guo, W. Xiao, M. Luo, Chem. Eng. Sci. 66 (2011) 4722–4732.